DENTAL MATERIALS 35 (2019) 1082–1094

Available online at www.sciencedirect.com

ScienceDirect

journal homepage: www.intl.elsevierhealth.com/journals/dema

Silane reactivity and resin bond strength to lithium disilicate ceramic surfaces

Maria Dimitriadi[a], *Maria Zafiropoulou*[a], *Spiros Zinelis*[a], *Nick Silikas*[b], *George Eliades*[a,*]

[a] *Department of Biomaterials, School of Dentistry, National and Kapodistrian University of Athens, Greece*
[b] *Biomaterials Unit, Dentistry, School of Medical Sciences, University of Manchester, UK*

ARTICLE INFO

Article history:
Received 16 March 2019
Received in revised form
23 April 2019
Accepted 3 May 2019

Keywords:
Silane reactivity
NMR
IR
Ceramic roughness
Resin bonding
Glass ceramic

ABSTRACT

Objective. To evaluate the silane status in commercially available products and their bonding capacity with polished glass-ceramic surfaces before and after hydrofluoric (HF) acid-etching.

Methods. The products tested were Calibra Silane Coupling Agent/CS, G-Multi Primer/GM, Kerr Silane Primer/KS, Monobond Plus/MB and Scotchbond Universal Adhesive/SB. The silane status was studied by ^{13}C nuclear magnetic resonance spectroscopy (^{13}C-NMR). The roughness parameters of polished (group A) and HF acid-etched (group B) lithium disilicate glass-ceramic surfaces were measured by optical profilometry (n = 5/group). The interaction of the products with group A and B ceramic surfaces was examined by attenuated total reflection Fourier transform infrared spectroscopy (ATR-FTIR). The shear strength (SBS) of a flowable composite bonded to the ceramic surfaces (groups A, B) was assessed before (NS) and after silane treatment (n = 20/group, product).

Results. The NMR analysis showed the presence of silanol monomers only in CS. Methoxylated-siloxane adducts were found in GM, silanol–siloxane adducts in MB, SB, and siloxane polymers in KS. Acid-etching greatly increased Sa, Sz, Sdr, Sc and Sv parameters ($p < 0.001$) and ATR-FTIR analysis demonstrated evidence of bonding with the substrate in CS. Weibull analysis of SBS revealed the following rankings in characteristic life ($p < 0.05$): CS > SB,KS,MB > GM > NS (group A) and CS > GM > SB,KS,MB,NS (group B). The most reliable treatment in both groups was CS. For the same silane treatment, the SBS of group B were significantly higher from group A. Failures were mainly of adhesive type, except of several partial resin cohesive failures found in group B.

Significance. The chemical bonding capacity of the silanes was highest in products with silanol monomers. Acid-etching increased bond strength to a level that neutralized the silane contribution in products with silanol–siloxane adducts and siloxane polymers, providing thus bond strength values similar to silane-free treatments.

* *Corresponding author at*: Department of Biomaterials, School of Dentistry, National and Kapodistrian University of Athens, 2 Thivon Str, Goudi, 115 27 Athens, Greece.
E-mail address: geliad@dent.uoa.gr (G. Eliades).
https://doi.org/10.1016/j.dental.2019.05.002

1. Introduction

Bonding of etchable glass-ceramics to tooth structure is highly important for the proper functional performance and longevity of the restoration-tooth complex, as it increases the ceramic strength [1,2] and seals the critical material-tissue interface [3].

Hydrofluoric (HF) acid-etching combined with silane primer treatments has been documented as the standardized protocol for bonding these restorations employing resin composite luting agents [4]. Although there are variations in the proposed HF acid concentrations, etching times and silane types [2,5], this procedure strengthens the interface by two synergistic bonding mechanisms: first, micromechanical retention, by infiltration of resin tags into the ceramic porosities created by the selective acid dissolution of the amorphous silica glass phase, and second, chemical adhesion, by condensation of the silanol groups of activated silane with the hydroxylated silica groups of the acid-etched ceramics, which is further stabilized via silanol intermolecular condensation [4]. Typically, HF concentrations of 5–10 wt% have been used in combination with dilute (2–5 wt%) alcoholic solutions of γ-methacryloxypropyl trimethoxysilane (MPTMS), either as a two-bottle system for hydrolytic activation prior to application or as a single-bottle prehydrolyzed form, ready for use.

During the last years, a variety of silane primers have been marketed composed of single-bottle silane mixtures with conventional or adhesive dental monomers and silane-containing universal dental adhesive formulations, despite the known instability of silanes in the presence of −OH containing compounds, polar groups and water [6,7]. Currently there is growing evidence that silanols are polymerized in such primers and adhesives [8–14].

The dual bonding mechanism of resin composites to acid-etched and silane primed glass-ceramic surfaces, has raised questions on the extent of the contribution of each individual treatment to the overall interfacial strength. Only in a few number of studies this issue has been addressed, but with contradictory findings; in two studies the status of the surface (polished or HF acid-etched) has been shown to have a negligible effect, considering the silane as the determinant factor [15,16], whereas in two other studies the opposite has been documented [17,18].

Currently, new silane containing primers and adhesives have been introduced with complex chemistry. The aim of the study was to assess the status of silane in water-free universal primers and a water-containing universal adhesive, to evaluate the reactivity of these products with polished and HF acid-etched glass-ceramic surfaces and to assess the bond strength of a resin composite to these surfaces, as mediated by the silane containing products. The hypotheses tested were: a) all the products contain active silanol groups, b) all the products have similar reactivity to polished and HF acid-etched surfaces, and c) the universal primers and adhesive provide higher strength than a conventional prehydrolyzed silane under both ceramic surface conditioning modes.

2. Materials and methods

The products used in the study are listed in Table 1. The silane status in the product vials was investigated by ^{13}C nuclear magnetic resonance spectroscopy (^{13}C-NMR), the roughness of the glass-ceramic specimens and their reactivity with the silanes were assessed by optical profilometry and micro-attenuated Fourier transform infrared spectroscopy (ATR-FTIR) respectively, whereas the bond strength of a resin composite to these surfaces as mediated by the silanes was evaluated under shear loading in a universal testing machine.

2.1. Silane status

Aliquots (0.5 mL) of each silane product were dried under nitrogen gas and the residue was dissolved in 0.45 mL deuterated dimethyl sulfoxide (DMSO-d_6). Samples of reference compounds (0.05 mL of non-hydrolyzed MPTMS, Evonik Industries, Darmstadt, Germany and 22 mg of 10-MDP, Ivoclar Vivadent) were dissolved as above. ^{13}C-NMR spectra of freshly prepared samples were acquired on a Bruker Avance DRX 500 MHz spectrometer (Bruker Biospin, Rheinstetten, Germany) equipped with a broad band probe and Topspin 1.3 software (Bruker Biospin). The spectral acquisition parameters were: number of scans = 6000, scan width = 250 ppm, 90° pulse = 12 μs, T = 298 °K. The signal of the solvent (DMSO-d_6) at 39.5 ppm was used for scale calibration. The α-CH_2 peak to the originally methoxylated Si atom of MPTMS [$-CH_2$–Si– $(OCH_3)_3$] was used to evaluate the hydrolysis status of the silane in the products tested. This peak demonstrates the greatest width of peak splitting in comparison with the other CH_2 peaks of the oxypropyl chain and has been proposed as the most appropriate for monitoring the silane hydrolysis process of MPTMS within the range of 7–11 ppm [19]. The experiment was replicated in triplicate.

2.2. Ceramic roughness

Cylindrical ceramic specimens (radius-r = 2.5 mm, height-h = 10 mm) were fabricated and embedded in epoxy resin leaving the top cyclical surface free. All specimens were polished with SiC papers (320–2500 grit-size) in a grinding-polishing machine (Dap-V, Struers, Ballerup, Denmark) under water coolant and ultrasonicated for 5 min in distilled water. Two specimen groups (A, B) were prepared (n = 5/group). In group A the polished specimen surfaces were left intact, whereas in group B, the surfaces were acid-etched with the HF-acid gel, left to react for 20 s, rinsed with water for 30 s and dried with oil-free dry air for 10 s. The surfaces were examined by an optical profiler (Wyko NT1100, Veeco, Tuscon, AZ, USA) under vertical scanning imaging mode, 2 mm scanning length, 40× magnification, 113.3 × 148.5 μm^2 analysis area, 2% modulation and tilt correction with 0.1 nm (z-axis) and 0.2 μm (x-, y-axis) resolution. The surface roughness parameters measured were the Sa, Sz (amplitude), Sdr (hybrid) and Sc, Sv (functional). On each specimen three measurements were performed and averaged, yielding the representative value.

Table 1 – The materials used in the study.

Product	Code	Composition[a]	Manufacturer
Glass-ceramic			
IPS e.max Press	–	SiO_2, Li_2O, K_2O, P_2O_5, ZrO_2, ZnO, Al_2O_3, MgO, La_2O_3 and pigments	Ivoclar Vivadent, Schaan, Liechtenstein
Ceramic etchant			
IPS ceramic etching gel	–	5% HF acid, colorants	Ivoclar Vivadent, Schaan, Liechtenstein
Silane agents			
Calibra Silane Coupling Agent	CS	MPTMS, Ethanol, Acetone	Dentsply Caulk Milford, DE, USA
G Multi Primer	GM	MPTMS, 10-MDP, MDTP, BisGMA, TEGDMA, Ethanol	GC Corp., Tokyo, Japan
Kerr Silane Primer	KS	MPTMS, BisEMA, TEGDMA, Ethanol	Kerr Italia, Scafatti, Italy
Monobond Plus	MB	MPTMS, 10-MDP, Disulfide dimethacrylate, Ethanol	Ivoclar Vivadent, Schaan, Liechtenstein
Scotchbond Universal Adhesive	SB	MPTMS, 10-MDP, 2-HEMA, BisGMA, DCDMA, VP-copolymer, SiO_2, Ethanol, Water, Initiators	3M ESPE, Neuss, Germany
Resin composite			
G-aenial Flo Universal	–	UEDMA, TEGDMA, BisEMA, 200 nm Sr-glass, 16 nm SiO_2 (69 wt%, 50 v%)	GC Corp, Tokyo, Japan

[a] According to the manufacturers' information. MPTMS: γ-methacryloxypropyl trimethoxysilane, 10-MDP:10-methacryloyloxydecyl dihydrogenphosphate, MDTP: methacryloyloxydecyl dihydrogen thiophosphate, BisGMA: bisphenol-A glycidyl dimethacrylate, TEGDMA: triethyleneglycol dimethacrylate, BisEMA: ethoxylated bisphenol-A dimethacrylate, 2-HEMA: 2-hydroxyethyl methacrylate, DCDMA: decamethylene dimethacrylate, VP-copolymer: methacrylate-modified polyalkenoic acid copolymer, UEDMA: urethane dimethacrylate.

2.3. *Ceramic reactivity with silanes*

Ceramic specimens (r = 2.5 mm, h = 2 mm) were prepared and polished as before. The specimens were carefully demolded and classified in two groups; in group A the specimens received no further treatment, while in group B they were acid-etched as previously described. On three specimens of each group the silane primers (CS,GM,KS,MB) and the adhesive (SB without irradiation) were applied as instructed, whereas three specimens with no silane treatment (NS) served as controls per group. All the specimens were stored under dark conditions (1 h/37 °C/70% RH). Then the treated surfaces were air-dried for 2 min to remove the loosely bound monomer fractions and analyzed by ATR-FTIR spectroscopy. A single reflection ATR accessory (Golden Gate, Specac, Orpington, UK) with type III diamond crystal and a p-oriented ZnSe grit polarizer was attached to a spectrometer (Spectrum GX, Perkin-Elmer, Buckinghamshire, UK), specimen surfaces were pressed against the crystal by a sapphire anvil and spectra were recorded as follows: 4000–650 cm^{-1} wavenumber range, 4 cm^{-1} resolution, 30 scans co-addition. Since the spectra of ceramic surfaces demonstrated peaks at the 1250–650 cm^{-1} band range, subtraction techniques were employed. Transmission spectra of primers and adhesive films applied on Ge windows prepared and stored as above, were used as reference. The presence of silanols (Si—OH, 904 cm^{-1}) in the films applied (groups A, B and reference) was further investigated by curve-fitting the second derivative peaks at the 1850–850 cm^{-1} region, employing Pearsons VII algorithm at standard width/variable shape mode and 2% zero baseline. Peak fitting analysis was performed by PeakFit v4.12 software (Seasolve, Framingham, MA, USA).

2.4. *Bond strength*

Two groups of the glass-ceramic specimens (A: polished, B: HF acid-etched, n = 20/group) were prepared as previously described for each silane containing material and the non-silane treated control. At the central part of each specimen a masking tape was placed, leaving a free circular area (r = 1.5 mm) for bonding. The designated surfaces of both groups were treated with the silane primers or the adhesive (thin film application with a microfiber brush, 60 s reaction period, 10 s air-drying). The specimens with the adhesive (SB) were irradiated for 10 s with a light-emitting diode curing unit (Radii Plus, SDI, Bainswater, Victoria, Australia) operated in standard mode (1500 mW/cm^2 light intensity). Cylindrical ring-shaped polyacetal molds (internal r = 1.5 mm, external r = 2 mm, h = 2 mm) were placed over the treated surfaces, filled with a single layer of the light-cured flowable composite (A2 shade) and irradiated for 30 s with the light curing unit. All molded specimens were stored in distilled water (7 days/37 °C) and then debonded under shear loading, applied at the ceramic-composite interface with the notched-edge blade method. A universal testing machine (Tensometer 10, Monsanto, Swindon, UK) was employed, operated at 1.0 mm/min crosshead speed. Fracture loads were divided by the nominal bonding surface area of the glass-ceramic specimens (πr^2) and the results of the shear bond strength (SBS) were expressed in MPa (N/mm^2). The debonded ceramic surfaces were subjected to failure mode analysis under a stereomicroscope (M80, Leica Microsystems, Wetlzar, Germany) at 10× magnification and a light microscope (DM 4000B, Leica Microsystems) operated in reflection at 50× magnification. Failure mode was classified as Type I (adhesive at the ceramic-composite interface), Type II (cohesive within the composite) Type III (mixed of type I and II) and type IV (cohesive within the ceramic).

2.5. *Statistical analysis*

Since the roughness data failed to pass normality or equal variance tests, a Mann–Whitney test was used to assess the statistically significant differences in roughness parameters between the two groups (polished vs acid-etched). For the

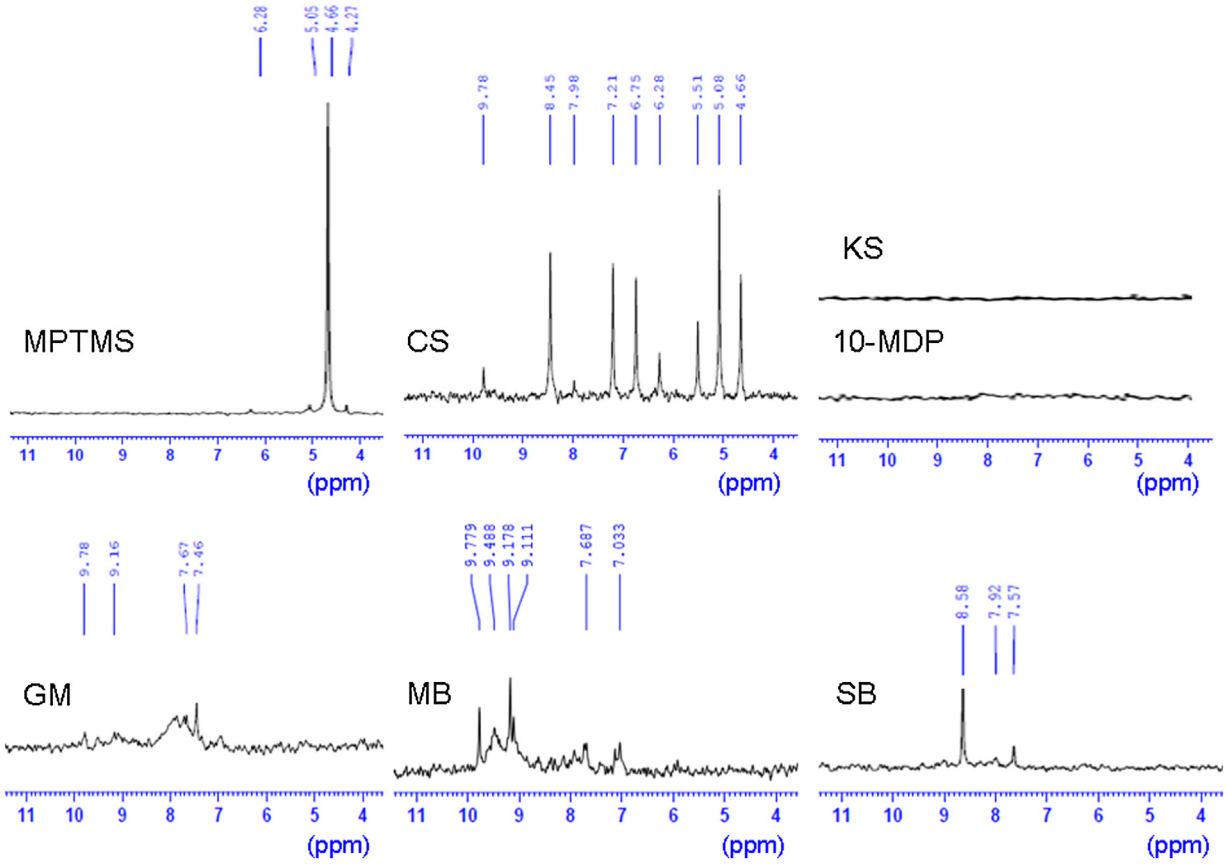

Fig. 1 – ^{13}C-NMR spectra of the silane containing materials and the controls (MPTMS, 10-MDP) at the 4–11 ppm region, associated with the MPTMS hydrolysis products. Peak annotations are listed in the text.

results of the SBS study, a Weibull analysis was performed. The shape or modulus parameter-β (defines the variability of the results, by expressing the size distribution of the flaws), the scale (σ_0) or B63.2 parameter, (defines the characteristic life, by indicating the strength value for which the 63.2% of the sample size were debonded) and the strength at 5% failure probability ($\sigma_{0.05}$) of the Weibull distributions were calculated. A Chi-square test was used to analyze the failure mode for each group and a two-way ANOVA (parametric general linear model) to evaluate the differences in percentages of type I (adhesive) failure modes per material and group. Finally, a Spearman test was executed to assess the correlation between the σ_0, $\sigma_{0.05}$ and the percentages in the type I failure modes. The statistical analyses for roughness, and failure mode were performed by SigmaStat software (SigmaPlot v.12.5, Systat Software Inc, San Jose, CA, USA). For the Weibull analysis the OriginLab software (v9.1 SRO, Northampton, MA, USA) was used. For all cases, a 95% confidence level was selected ($\alpha = 0.05$).

3. Results

3.1. *Silane status*

Fig. 1 demonstrates representative ^{13}C-NMR spectra of the silane containing products and controls at the α-CH_2 region (4–11 ppm). No peaks appeared in the spectrum of 10-MDP, since the first peak (methacrylate CH_3 group) was located at 18.4 ppm. The reference, non-hydrolyzed MPTMS, showed a very strong peak at 4.7 with very small peaks at 4.2, 5.1 ppm assigned to the methoxy groups [–Si–(OCH_3)] and a small peak at 6.2 ppm, attributed to a minor hydrolyzed fraction. The prehydrolyzed CS demonstrated a peak at 4.7 ppm of non-hydrolyzed methoxy groups and an array of peaks which correspond to partially hydrolyzed and condensed species of the chemical structure $-CH_2-Si-(OCH_3)_{3-n}(OH)_{n1}(O-Si-CH_2-)_{n2}$. Based on the annotation proposed in a previous study [19], the peak at 6.9 ppm may correspond to mono-silanols (n = 2, n1 = 1, n2 = 0), the peak at 7.2 to di-methoxy, siloxane dimers (n = 2, n1 = 0, n2 = 1), the peak at 8.0–8.3 ppm to di-silanols (n = 1, n1 = 2, n2 = 0), the peak at 8.5 ppm to mono-methoxy, mono-silanol siloxane dimers (n = 1, n1 = 1, n2 = 1) and the peak at 9.7 ppm to di-silanol siloxane dimers (n = 3, n1 = 2, n2 = 1). The peaks at 5.1 and 5.5 ppm were not identified. However, as they resonate at lower fields, they could be assigned to silanol hydrolysis intermediates. No fully hydrolyzed methoxy groups were detected (tri-silanols), which are probed at 9.5 ppm. The spectrum of GM showed broad and small peaks at the 7–8 ppm region, indicating the presence of methoxylated dimers (7.4 ppm). No peaks were traced in the KS spectrum at the 4–11 ppm region. In MB spectrum, small and broad peaks were identified at the 9–10 ppm region, confirming the presence of residual silanol activity in the condensates formed

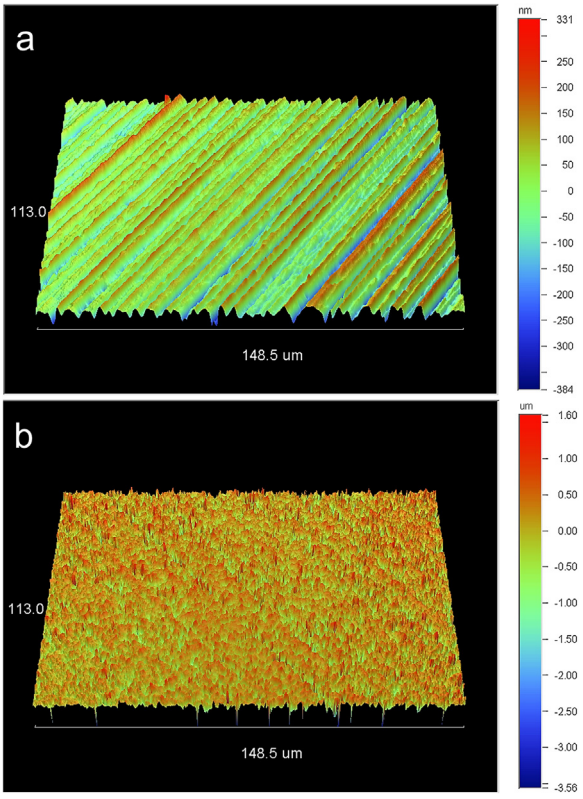

Fig. 2 – 3D-profilometric images of polished (a; 331 to −384 nm scale range) and acid-etched surfaces (b; 1.60 to −3.65 μm scale range). Note that the scale range in b is approximately eight times greater than in a (40× magnification).

(dimers, etc.). In SB spectrum, the 8.5 ppm peak complies with the formation of incompletely hydrolyzed mono-silanol siloxane dimers, with residual silanol activity.

3.2. *Ceramic roughness*

3D-profilometric images of the polished and acid-etched surfaces are illustrated in Fig. 2. The results of the roughness parameter measurements are presented in Table 2. The acid-etched specimens demonstrated a statistically very significant increase in all the roughness parameters tested ($p < 0.001$). The most affected parameter was the Sdr (~55× increase), whereas the increase in the values of the other parameters tested ranged between 3–6×.

3.3. *Ceramic reactivity with silanes*

ATR-FTIR spectra of the non-silanated control surfaces are illustrated in Fig. 3. Acid-etching reduced the peaks at 1237, 1111, 990 cm^{-1} (Si–O–Si asym), 958 (Si–O–Si of SiO_4 tetrahedra) and 785, 756 cm^{-1} (Si–O–Si sym) [20] of polished surfaces. Moreover, the strong and broad Si–O–Si peaks of the polished specimens at 991 and 910 cm^{-1} became sharper and shifted +20 cm^{-1} towards higher wavenumbers, possibly indicating increased crystallinity of the acid-etched structure [21]. The peak at 844 cm^{-1} was not traced in acid-etched specimens. Subtraction ATR-FTIR (D: primed minus the corresponding polished or acid-etched surfaces) and reference transmission FTIR spectra for each silane agent are depicted in Figs. 4–8. For CS, the subtraction spectra on both substrates were similar to the reference at the 1800–1150 cm^{-1} region (Fig. 4), except the increased intensity of the peak at 1699 cm^{-1} (H-bonded resonance stabilized carbonyl groups) in the polished sample and the peaks at 1253 cm^{-1} in the polished and acid-etched samples, which probably are the longitudinal phonon peaks (LO) of silane Si–O– groups bonded to the glass-ceramic substrate [22]. At the 1150–900 cm^{-1} region the polished specimen demonstrated a broad peak at 1078 cm^{-1} (Si–O–C) with high and low band shoulders at 1120 and 1015 cm^{-1} (Si–O–Si). The peak at 1120 cm^{-1} appeared also in acid-etched specimens with an additional one at 1095 cm^{-1}, the latter possibly attributed to chemisorbed silane [23]. The spectra of GM and MB (Fig. 5 and 6) demonstrated Si–O–Si peaks in polished and acid-etched specimens (1125, 1097 and 1016 cm^{-1}). In reference and polished GM specimens and in reference and acid-etched MB specimens, additional peaks were identified at 1247 (P═O) and 1038 cm^{-1} (P—O—C) assigned to the phosphate monomers. For KS with aliphatic (C═C str, 1638 cm^{-1}), aromatic (C···C str, 1605 cm^{-1}) and urethane (N—H str, 1540 cm^{-1}) resin monomers (Fig. 7), no substantial peak differences were found in treated surfaces, except a small increase of the peak intensity at 1125 cm^{-1} (Si–O–Si) on polished and acid-etched specimens. The spectra of SB showed similar peaks associated with the 10-MDP, silane and possibly colloidal silica particles (Fig. 8). The 1040–1012 cm^{-1} band (Si—O—Si plus P—O—C vibrations) manifested the highest absorbance on polished and the lowest on acid-etched specimens. A reduction in the peak intensity ratio (R) of the aliphatic C═C (1638 cm^{-1}) to the aromatic C···C (1605 cm^{-1}) bonds was registered on acid-etched (R = 1.1) vs polished and reference specimens (R = 1.7–1.8). The reference SB spectrum demonstrated peaks at 1744 cm^{-1} (−COOH), which were traced only in the acid-etched specimen, whereas peaks of carboxylate salts (−COOM, 1540 cm^{-1}) were probed on the acid-etched specimens. Curve-fitting revealed Si−OH peaks only in CS and MB reference films (Fig. 9).

3.4. *Bond strength*

The results of the Weibull analysis (β, σ_0, 95% C.I. for σ_0, $\sigma_{0.05}$ and 95% C.I for $\sigma_{0.05}$) are listed in Table 3. For group A specimens, the ranking of reliability (β), from highest to lowest, was CS,KS,SB,MB,GM,NS ($p > 0.05$), whereas the ranking of statistically significant differences in characteristic life (σ_0) was CS > SB,KS,MB > GM > NS ($p < 0.05$). For group B specimens the corresponding rankings were CS,SB,NS > KS > MB,GM in β and CS > GM > SB,KS,MB,NS in σ_0 ($p < 0.05$). The $\sigma_{0.05}$ relative to σ_0 ranged between 50–67% in group A and 40–60% in group B. In both groups, CS showed the highest $\sigma_{0.05}$ within a statistically homogeneous ranking ($p > 0.05$) with KS, SB (group A) and SB (group B).

Since the roughness measurements showed a high increase (~55×) in percentage surface area after acid-etching, the σ_0 and $\sigma_{0.05}$ group ratios (B/A ratios) were calculated to justify the role of acid-etching. For the NS control, HF acid-etching increased the σ_0 values by a factor of 10.5 in comparison with the polished control. For the silane treatments GM demon-

Table 2 – Results of the roughness parameters tested (median values and 25%–75% percentiles in parentheses). Same superscripts show median values with no statistically significant difference per parameter (p > 0.05).

Group	Sa (nm)	Sz (μm)	Sdr (%)	Sc (nm^3/mm^2)	Sv (nm^3/mm^2)
A (polished)	85.5^{a} (7.7–9.5)	0.7^{a} (0.7– 0.8)	1.2^{a} (1.2–1.7)	117.8^{a} (109.1–131.6)	13.1^{a} (11.8–13.9)
B (acid-etched)	310^{b} (275.1–380.6)	3.9^{b} (3.6–4.3)	66.5^{b} (51.1–100.3)	385.3^{b} (329.7–483.9)	64.3^{b} (61.7–73.1)

Sa: The arithmetic average of the absolute values of the surface height deviations measured from the best fitting plane.
Sz: The 10 point height over the surface, representing the average difference between the 5 highest peaks and 5 lowest valleys.
Sdr: The developed area due to the surface texture versus an ideal plane area ratio.
Sc (core void volume): The volume supported by the surface from 10% to 80% of the bearing ratio.
Sv (surface void volume): The volume the surface would support from 80% to 100% of the bearing ratio.

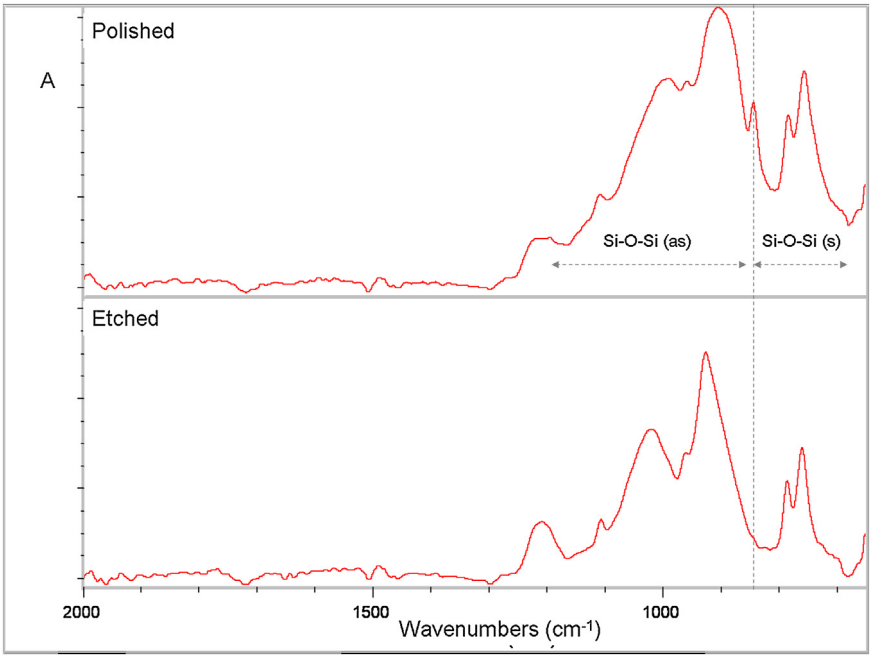

Fig. 3 – ATR-FTIR spectra of the polished and acid-etched glass-ceramic surfaces (2000–650 cm^{-1} range).

Table 3 – Results of the shear bond strength test and percentage of adhesive failures.*

Treatment	Weibull β-parameter	Weibull σ_0 (95% C.I.) MPa	Weibull r^2 σ_0	Weibull $\sigma_{0.05}$ (95% C.I.) MPa	Adhesive failures (%)
Group A: polished					
CS	7.1^{a} (5–9.9)	6.4^{a} (6–6.8)	0.98	4.2^{a} (3.1–5)	100
GM	$4.5^{a,e}$ (3.1–6.2)	3.2^{b} (2.9–3.6)	0.96	1.7^{b} (1.3–2)	100
KS	7.0^{a} (4.7–8.8)	4.7^{c} (4.3–5)	0.96	$3.1^{a,c}$ (2.3–3.7)	100
MB	$4.3^{a,g,h,i}$ (2.7–5.1)	4.2^{c} (3.8–4.7)	0.93	$2.1^{b,c}$ (1.3–2.8)	100
SB	$5.5^{a,j,k,l}$ (3.7–7.3)	4.8^{c} (4.4–5.2)	0.94	$2.8^{a,c}$ (1.9–3.5)	100
NS	$4.9^{a,m,n,o}$ (2.9–5.5)	2.3^{d} (2.1–2.5)	0.88	1.2^{b} (0.8–1.6)	100
Group B: acid-etched					
CS	$6^{a,b}$ (4.3–8.5)	48.4^{e} (44.2–52.7)	0.96	28.9^{d} (21.1–36.1)	40
GM	$3.4^{d,g,j,m}$ (2.1–4.2)	36.8^{f} (31.8–42.4)	0.85	$14.8^{d,e}$ (8.1–21.7)	55
KS	$3.3^{c,f,h,k,n}$ (2.4–4.9)	25.7^{g} (21.9–29.7)	0.95	10.4^{e} (5.6–15.2)	65
MB	$3.3^{d,e,i,l,o}$ (2.2–4.3)	24.9^{g} (21.3–28.4)	0.91	10.3^{e} (5.5–14.9)	55
SB	$5.5^{a,b}$ (4–7.9)	28.5^{g} (25.9–31.5)	0.96	16.5^{e} (11.5–20.6)	70
NS	$4.4^{a,b}$ (2.7–5.2)	24.1^{g} (21.7–27.5)	0.88	12.5^{e} (7.7–12.6)	90

* Same superscripts show mean values with no statistically significant differences (p > 0.05).

strated the highest ratio (11.5), followed by CS (7.6) and the group of KS,MB,SB (5.5–5.9). Regarding the $\sigma_{0.05}$ value ratios, NS demonstrated the highest ratio (10.4), followed by the silane treated groups GM (8.7), CS (6.9), SB (5.9), MB (4.9), and KS (3.4). In two treatments (NS, SB) the $\sigma_{0.05}$ value ratios were similar to σ_0.

Representative images of the debonded ceramic surfaces are presented in Fig. 10. The results of the failure mode analysis are summarized in Table 3. For group A specimens,

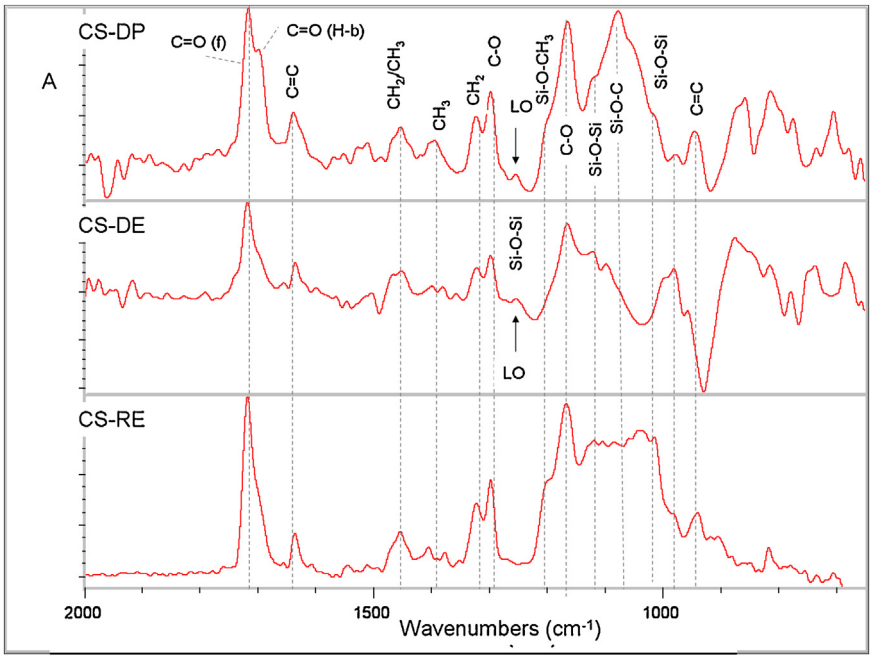

Fig. 4 – Transmission spectra of reference CS film (RE) and difference ATR-FTIR spectra of the film formed on polished (DP) and acid-etched (DE) glass-ceramic surfaces. Arrows show the LO peaks (2000–650 cm^{-1} range).

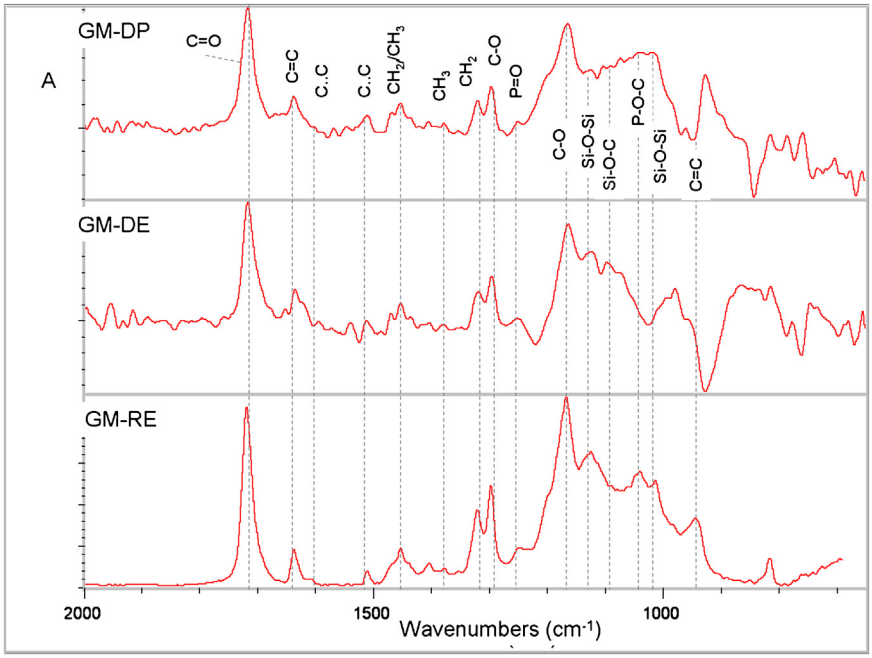

Fig. 5 – Transmission spectra of reference GM film (RE) and difference ATR-FTIR spectra of the film formed on polished (DP) and acid-etched (DE) glass-ceramic surfaces (2000–650 cm^{-1} range).

typical adhesive failures (type I) were observed (Fig. 10a), with sporadic cases of minimal adhesive film remnants, as in SB (Fig. 10b). For group B specimens, the failure modes were of type I and III. Type III failures, included thin residual films covering the debonded ceramic surface area up to 25% (Fig. 10c–e) and two cases of cohesive composite failures with fracture striations located opposite to the loaded part (Fig. 10f). There were no statistical significant failure mode difference in group A (all type I) and B (type I and III, Chi-square = 9.52, $p = 0.09$). The analysis of the percentage type I failures per silane and surface conditioning treatment showed that a significant effect was exerted only by the surface conditioning treatment (polished vs acid-etched, $p = 0.007$) and not by the silane type, including the NS group ($p = 0.33$). The Spearman's correlation coefficient showed a non-significant correlation between σ_0, $\sigma_{0.05}$ and type I failure mode in group B

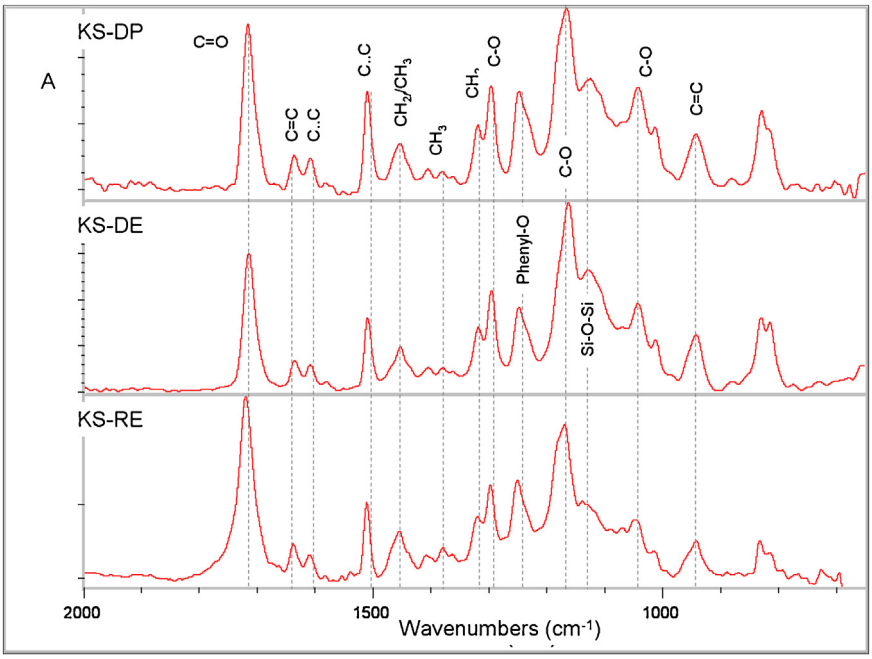

Fig. 6 – Transmission spectra of reference KS film (RE) and difference ATR-FTIR spectra of the film formed on polished (DP) and acid-etched (DE) glass-ceramic surfaces (2000–650 cm^{-1} range).

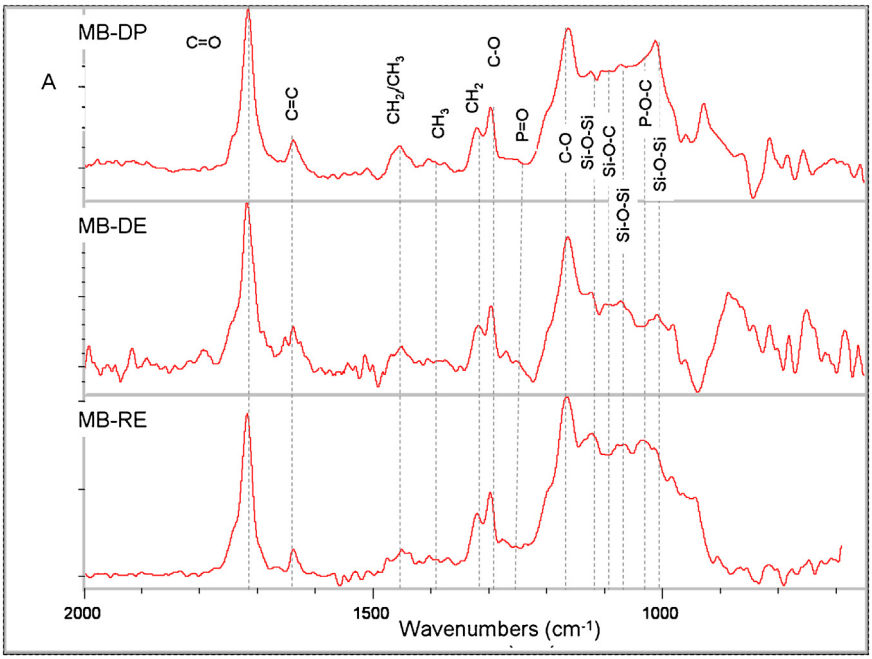

Fig. 7 – Transmission spectra of reference MB film (RE) and difference ATR-FTIR spectra of the film formed on polished (DP) and acid-etched (DE) glass-ceramic surfaces (2000–650 cm^{-1} range).

($r = -0.67$, $p = 0.14$ and $r = -0.23$, $p = 0.66$ respectively). However, when the data of groups A and B were merged, a very significant correlation was found ($r = -0.90$ and $r = -0.84$ respectively with $p < 0.0001$).

4. Discussion

The results of the present study showed that silanol monomers were mainly detected in the prehydrolyzed primer. Some residual silanol activity was identified in a universal

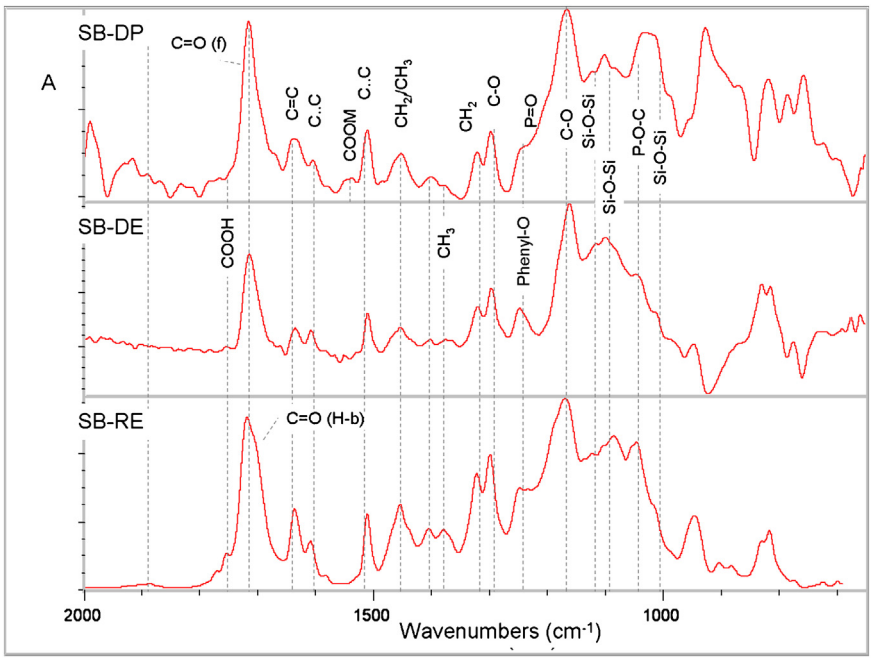

Fig. 8 – Transmission spectra of reference SB film (RE) and difference ATR-FTIR spectra of the film formed on polished (DP) and acid-etched (DE) glass-ceramic surfaces (2000–650 cm^{-1} range).

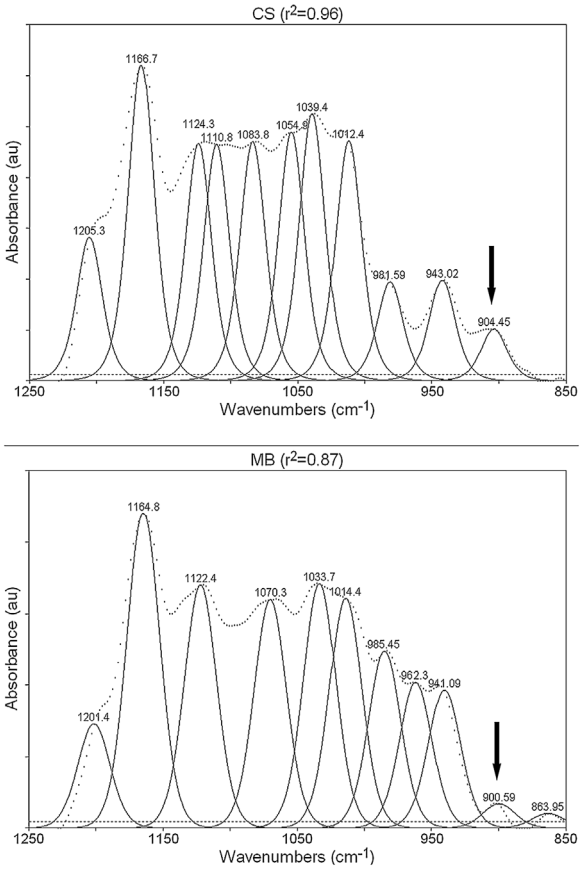

Fig. 9 – Curve fitting of the transmission spectra of reference CS and MB films. Arrows show the peak of silanols (1250–850 cm^{-1} range).

silane primer and the adhesive. Therefore, the first hypothesis should be partially rejected. The second hypothesis should be also rejected, since there were differences in the reactivity of the silanes with polished and acid-etched ceramic surfaces, with the exception of KS. Finally, the third hypothesis should be also rejected since none of the primers or the adhesive tested resulted in higher strength than the conventional prehydrolyzed silane primer, under the surface conditioning modes evaluated.

The results of the present study are in agreement with previous studies on the status of the MPTMS silane contained in water-free primers [12,14] and water containing adhesives [10,13,14]. In most materials condensates were found, with reduced activity, as documented by the chemical shifts and the low, broad peak intensities in the ^{13}C-NMR spectra. The only primer containing clearly resolved silanol monomers was CS. The detection of residual methoxy groups in the prehydrolyzed primer, due to incomplete hydrolysis, supports previous findings [14,24].

Silane interactions with –OH and polar-group containing monomers have long been considered as the reason for silanol deactivation [6,7]. The extent of this reaction was mostly pronounced in KS, where no silane peaks were identified at the 4–11 ppm region, possibly due to formation of silyl-ether monomer derivatives with BisGMA [14] and silsesquinoxanes with polar TEGDMA and BisEMA monomers, possessing ^{13}C shifts ≫11 ppm. The water-free silane primers, GM and MB, showed no evidence of methoxy groups (4.7 ppm), as the silane in these products may react with adhesive and conventional monomers, reaching an equilibrium of hydrolyzed and condensed phases. The shifting of the MB broad peaks at higher fields than GM implies the presence of more condensed species in the former. The silane in SB appeared almost in a

single phase, partially condensed. It seems that the acidic pH of the adhesive (pH 2.7) in the presence of water, pronounced the condensation of the hydrolysates to a certain extend.

The significant increase in all roughness parameters after acid-etching has been clearly documented in the present study. The very high increase in the surface area (Sdr) and the volume retention capacity per area unit (Sc, Sv) indicate that the acid-etched surfaces are highly retentive, provided that the adherent resin composite has a proper balance of viscosity and surface tension for adequate ceramic infiltration. The greater Sv value ratio of acid-etched vs polished specimens (4.9) in comparison with the corresponding Sc ratio (3.3), implies that Sv is more pronounced after acid-etching.

For the study of the silane chemical reactivity, an environmental surface sensitive method was chosen (ATR-FTIR), since the rapid removal of the volatile reaction products (methanol in MPTMS) by high vacuum techniques, could shift the reaction equilibrium towards siloxane formation. In addition, flat surfaces instead of powders were used to better simulate the clinical analogue, since powders with a very high surface area enhance any chemical reaction. By using a diamond ATR element and a p-polarizer, a higher effective path-length was established for the IR beam component parallel to the plane of incidence, which results in enhanced absorbance of vibrations within this plane rather than the perpendicular one [25].

Acid-etching increased the crystallization of the glass-ceramic structure, apparently by dissolving part of the weaker amorphous silica phase. In the subtraction spectra of all polished glass-ceramic surfaces, except KS, the Si–O–Si peaks were stronger in comparison with the acid-etched surfaces, suggesting a more pronounced siloxane network formation. The CS film on polished surfaces demonstrated a strong peak assigned to H-bonded resonance stabilized carbonyl groups (1699 cm^{-1}) relative to the non H-bonded (1720 cm^{-1}), indicating increased molecular orientation and surface adsorption [26,27]. Nevertheless, the complex Si–O– absorption patterns at the 1260–1000 cm^{-1} region make very difficult the identification of Si–O bonds at the silane/glass-ceramic interface from the silane Si–O–Si intermolecular bonds and the Si–O bonds of the ceramic. For this reason spectra subtraction techniques were employed, which have long been introduced for studying interaction of silanes with silica surfaces, since they demonstrate increased sensitivity for surface chemical treatments when the concentration of the functional groups involved is low [28]. It has been postulated that the peak at 1253 cm^{-1} of the subtracted ATR spectra, assigned to the longitudinal oriented phonon mode of Si–O–, is affected only by direct bonding of silane molecules with silica and not by silane polycondensation [22]. Therefore, it can be used to probe the silane-substrate interactions. For CS this peak, absent from the reference spectrum, was more prominent on the polished substrate. The increased reactivity of the polished substrate should be attributed to the increased glass content. No such peaks were identified in the subtraction spectra of the other silanes, since the peaks found at 1247–1243 cm^{-1} in the GM, MB, SB spectra, existed in the corresponding reference spectra as well, and were mainly due to the P=O vibrations of the phosphate monomers. The reduced amount of silanols available for bonding, because of silane interactions with other polar molecules as documented by the ^{13}C NMR analysis, corroborates the ATR findings. For KS, a negligible change in the Si–O–Si peak intensity was found on polished and acid-etched specimens relative to the reference, which confirms the minimal silanol activity in this primer. For SB, with more reactive silanols than KS, siloxane and P—O—C peaks were better resolved on polished surfaces. Also, on polished surfaces the original –COOH peak was diminished and –COOM peaks appeared, as a result of a secondary reaction of the methacrylate-modified polyalkenoic acid copolymer with basic oxides of the glass-ceramic surface. An interesting finding for the SB film formed on acid-etched surfaces, was that the region analyzed was deficient in aliphatic monomers by ~40% in comparison with polished surfaces and the reference. Apparently the high molecular weight hydrophobic aromatic monomer BisGMA failed to efficiently infiltrate the complex porous structure of the acid-etched glass ceramic, creating a surface zone rich in BisGMA, which was probed by the ATR analysis. Such phase separation phenomena have been already documented in single-bottle adhesives applied on phosphoric acid-etched dentin [29].

The main prerequisite for glass-ceramic silanization is to enhance the chemical bonding capacity of resin composites. Comparison of the silane bond strength values to polished substrates before and after acid-etching could provide a means of estimating the contribution of chemical bonding, when non-silanized treatments (NS) are used as controls. Nevertheless, such comparisons are difficult to interpret since the chemistry of a protonated and hydroxylated acid-etched glass-ceramic surface is different from a polished one, while concurrently, the bonding area is highly increased.

In the present study, a high-strength ultrafine particle-filled flowable light-cured resin composite has been used as the adherent material. This material demonstrates flexural strength and fracture toughness at the range of conventional paste composites [30], but at a flowable consistency. Since the strength of the adherent material is implicated in shear loading, as bending moments cannot be avoided [31], a strong restorative material was preferred rather than a weaker luting agent. Furthermore, the flowable consistency of the restorative, matching that of most resin composite luting agents, is equally important for a porous-free adaptation and proper infiltration of the complex acid-etched glass-ceramic surface morphology.

The SBS values to silanized polished surfaces may be considered as an indication of the chemical bonding achieved, because micromechanical retention was minimal due to the small roughness values. Despite the low values of group A, all silane treatments tested were stronger and more reliable than the NS control, supporting thus a means of chemical bonding. From the products tested in group A, CS was the strongest and most reliable, because of the availability of reactive mono- and di-silanol monomers for bonding with the substrate and bond stabilization via intermolecular crosslinking, as evidenced from the NMR and ATR studies. KS, MB and SB, were ranked next to CS in β and σ_0. Although these three products contain different states of MPTMS, according to the ^{13}C-NMR analysis, they also demonstrate different film properties (SB was separately polymerized, KS and MB were used as uncured primers) and different composition (KS: conventional monomers, MB: adhesive monomers, SB: conventional

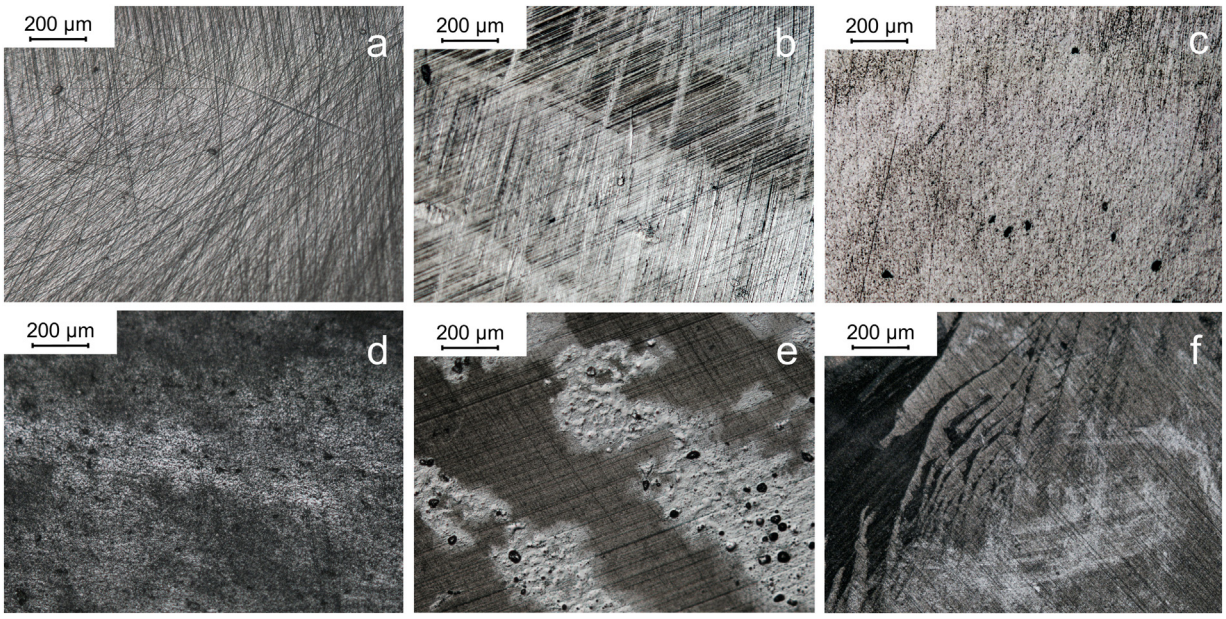

Fig. 10 – Representative reflected-light microscopic images of debonded ceramic surfaces from groups A (polished) and B (polished and HF acid-etched), with various types of failure modes (50×, bar = 200 µm).
a) Group A, typical adhesive composite failure; b) Group A, mainly adhesive composite failure with limited ceramic surface coverage by a residual film; c) Group B, typical adhesive composite failure; d, e) Group B, adhesive composite failure with more extended coverage by residual films; f) Group B, complex failure pattern including cohesive composite failure and partial ceramic surface coverage by resinous films.

and adhesive monomers plus filler thickeners). Therefore, it is not possible to exclusively assign their bonding capacity to the different silane states. Such comparisons, yet, can be made between MB and GM. Both these universal primers contain phosphate and sulfur functionalized monomers, which are not considered as efficient as silanes for bonding to glass-ceramics [18]. Consequently, the status of MPTMS could explain the statistically different strength between the two materials. The higher strength of MB could be explained by the residual silanol activity, contrary to the methoxylated dimers found in GM, which require further activation, not inducible by the polished glass-ceramic surfaces. This activity was documented, as well, by the curve-fitting analysis of the reference IR spectra and by the increased peak intensity at the 1040–1020 cm^{-1} region of ATR spectra vs the corresponding reference.

After HF acid-etching, the glass-ceramic surfaces were protonated and hydroxylated, conditions that enhance the in situ hydrolysis of MPTMS [32,33] and very rough, for increased micromechanical retention. The prehydrolyzed primer CS, again manifested the highest strength and reliability. An additional in situ hydrolysis of the unreacted methoxy groups of CS and subsequent chemisorption/intermolecular crosslinking of the produced silanols on the substrate may explain this performance, since micromechanical retention was common in all silane treated specimens and the control. For CS, the ATR analysis documented the presence of LO peaks on polished and acid-etched surfaces. It should be mentioned, though, that the surface area of the acid-etched specimens in contact with the flat ATR diamond crystal was strongly reduced due to the rough ceramic structure left after HF-etching, which exceeds the mean sampling depth of the ATR method (1–2 µm). Consequently, the information obtained corresponded to the fraction of the silanized ceramic surface protrusions in contact with the diamond crystal. GM, with residual methoxy groups as well, was ranked second to CS for the same reason, but with a fair reliability (β), possibly associated with the presence of siloxane derivatives in the vial. An interesting finding was the statistically insignificant differences in σ_0 between SB,KS,MB and the NS control. Apparently the variations in MPTMS phases, product composition and film properties, as previously discussed, had a negligible effect on the acid-etched substrate. It is also interesting that the reliability of NS was ranked third after CS and SB. It seems that, the viscosity and surface tension of the flowable composite used, created a micro-mechanical retention pattern capable of neutralizing the chemical contribution of the different silane phases to the bond strength. The remarkable reliability of SB (3rd in group A and 2nd in group B) should be related to the presence of a separately light-cured interfacial layer, with conventional and adhesive resin monomers plus the vinyl-copolymer. In contrast, KS, only with conventional monomers but no separate light-curing capacity, was the least reliable in group B, although ranked first in group A. This discrepancy may be ascribed to an inadequate polymerization of the KS fraction infiltrated into the complex porous ceramic structure, by either free radical or condensation reactions.

The $\sigma_{0.05}$ values, considered as more clinically relevant than σ_0 [34], showed higher reliability (β-parameter) in group A, which may be explained by the 100% type I failures (adhesive type) observed, without implications of the

ceramic and composite cohesive strengths with the interfacial strength. Nevertheless, the strength values in group B were much higher with cohesive failures of the resin composite, which highlights the clinical relevance of acid-etching in the $\sigma_{0.05}$ as well.

The B/A group σ_0 ratios were used as an indication of the strength enhancement induced by acid etching, For GM and the NS control, which demonstrated the lowest σ_0 values in group A, the ratios registered were the highest, implying the determinant role of acid-etching. The ratios were lowest in KS, MB, SB, where the σ_0 values in group A were ranked as intermediate, indicating that these silane primers were more effective as chemical coupling agents than GM. Finally, CS with the highest value in both groups exhibited an intermediate ratio, which supports an optimum combination of silane bonding and micromechanical retention. The ranking of the corresponding $\sigma_{0.05}$ ratios was similar to the σ_0 ratios and in two treatments (NS and SB) the $\sigma_{0.05}$ value ratios were similar to σ_0. The latter suggests that the 5% failure probability ratios may express the characteristic life ratios.

The results of failure mode analysis showed a complex type III pattern in many group B specimens. Some partial composite cohesive failures were observed at opposite directions to the loading sites. The characteristic fracture striations were mostly oriented vertically to the loading direction, as a result of the tensile stress vectors of the bending moments developed at the region [31]. The statistically insignificant differences in the failure modes within groups A and B imply that the type of the silane agent was not a significant factor. This was also confirmed by the 2-way ANOVA analysis of the type I failures in both groups, which revealed that the determinant factor was the type of the substrate.

The results of the present study showed that a prehydrolyzed MPTMS primer was more effective than MPTMS primers containing conventional or adhesive monomers and an MPTMS containing adhesive for resin bonding to a glass-ceramic.

This suggests that pure silane treatment should be advised as the silane coupling agent of choice for glass-ceramics. However, the clinical relevance of these results should be carefully interpreted, considering several limitations. The ^{13}C-NMR analysis performed provided information for the MPTMS status in freshly delivered product vials, without any storage-related aging effects. In the present study ^{13}C-NMR has been selected, since it has been considered as more appropriate for studying the initial states of the silane hyrolysis than ^{29}Si-NMR, which is best for identification of the species formed at the end of the condensation reaction [19]. The profilometric method used probed the superficial ~5 μm zone of the porous acid-etched specimens (maximum peak to valley range), with open orifices accessible to white-light fringe pattern. Apparently more complex topographies (i.e. subsurface pore extension, lateral pore interconnection, etc.) were not encountered in the measurements, although they may contribute to micromechanical retention. The ATR-FTIR study probed the entire surface in contact with the diamond crystal of polished specimens but only the superficial fraction of the acid-etched surfaces; hence, the findings may not represent the interaction pattern at regions distal to the depth of the evanescent wave formed. In addition it was not feasible to probe Si—O—Li bonds with the substrate as documented in a recent study [35] A macro-shear test was preferred, instead of the more popular micro-shear, since low strength values were expected in the groups without acid-etching. For such cases micro-shear tests are not indicated [36]. Moreover, specimens were not demolded to avoid premature failures from the associated stresses. The isothermal water storage at 37 °C for a week is a mild method of testing interfacial hydrolytic stability. Although frequently used in bond strength experiments, it may only provide the baseline for any aging condition (thermal- or load-cycling, etc.). Finally, an inherent limitation of the otherwise easy to perform SBS test, is the uneven interfacial stress distribution. However, the introduction of the notched-edge design has improved the stress distribution, providing hence a more standardized testing method [37].

5. Conclusion

Based on the results of the present study, the silane primers and adhesive tested contain various forms of MPTMS, including partially hydrolyzed silanol monomers, methoxy- and methoxysilanol-functionalized siloxane dimers and siloxane polymers. The primer with the silanol monomers demonstrated chemical bonding via the Si—O– groups with the substrate, whereas carboxylate salts were formed between the adhesive and the substrate. These reactions were more pronounced on polished surfaces. The primer with the silanol monomers showed the highest bond strength to polished and to acid-etched glass ceramic surfaces, with the highest reliability. The number of products with statistically significant differences in the characteristic life on polished surfaces was reduced after acid-etching, because of the contribution of the micromechanical retention. This reinforcement was quite strong to balance the reduced chemical bonding capacity of several products with reduced or minimal silanol activity.

Acknowledgements

We would like to thank Drs. A. Panagiotopoulou, M. Pelecanou and K. Yannakopoulou for the ^{13}C-NMR analysis (High Resolution NMR Lab, NCSR “Demokritos”, Ag. Paraskevi, Greece). This research is co-financed by Greece and the European Union (European Social Fund- ESF) through the Operational Programme «Human Resources Development, Education and Lifelong Learning» in the context of the project “Strengthening Human Resources Research Potential via Doctorate Research” (MIS-5000432), implemented by the State Scholarships Foundation (ΙΚΥ).

REFERENCES

[1] Scherrer SS, de Rijk WG, Belser UC, Meyer JM. Effect of cement film thickness on the fracture resistance of a machinable glass-ceramic. Dent Mater 1994;10:172–7.

[2] Xiaoping L, Dongfeng R, Silikas N. Effect of etching time and resin bond on the flexural strength of IPS e.max Press glass ceramic. Dent Mater 2014;30:e330–6.

[3] Christgau M, Friedl KH, Schmalz G, Resch U. Marginal adaptation of heat-pressed glass-ceramic veneers to dentin in vitro. Oper Dent 1999;24:137–46.

[4] Zohairy AE, Feilzer AJ. Bonding in prosthodontics with cements. In: Eliades G, Eliades T, Watts D, editors. Dental hard tissues and bonding, chapter 7. Heidelberg: Springer; 2005. p. 155–73.

[5] Puppin-Rontani J, Sundfeld D, Costa AR, Correr AB, Puppin-Rontani RM, Borges GA, et al. Effect of hydrofluoric acid concentration and etching time on bond strength to lithium disilicate glass ceramic. Oper Dent 2017;42: 606–15.

[6] Antonucci JM, Dickens SH, Fowler BO, Xu HH, McDonough WG. Chemistry of silanes: interfaces in dental polymers and composites. J Res Natl Inst Stand Technol 2005;110:541–58.

[7] Farahani M, Wallace WW, Antonucci JM, Guttman CM. Analysis by mass spectrometry of the hydrolysis/condensation reaction of a trialkoxysilane in various dental monomer solutions. J Appl Polym Sci 2006;99:1842–7.

[8] Lee Y, Chae M, Kim KH, Kwon TY. Effect of dental silane primer activation time on resin–ceramic bonding. J Adhes Sci Technol 2015;29:1155–67.

[9] Kim RJ, Woo JS, Lee IB, Yi YA, Hwang JY, Seo DG. Performance of universal adhesives on bonding to leucite-reinforced ceramic. Biomater Res 2015;19:11.

[10] Yoshihara K, Nagaoka N, Sonoda A, Maruo Y, Makita Y, Okihara T, et al. Effectiveness and stability of silane coupling agent incorporated in 'universal' adhesives. Dent Mater 2016;32:1218–25.

[11] Yao C, Zhou L, Yang H, Wang Y, Sun H, Guo J, et al. Effect of silane pretreatment on the immediate bonding of universal adhesives to computer-aided design/computer-aided manufacturing lithium disilicate glass ceramics. Eur J Oral Sci 2017;125:173–80.

[12] Pilo R, Dimitriadi M, Palaghia A, Eliades G. Effect of tribochemical treatments and silane reactivity on resin bonding to zirconia. Dent Mater 2018;34:306–16.

[13] Yao C, Yu J, Wang Y, Tang C, Huang C. Acidic pH weakens the bonding effectiveness of silane contained in universal adhesives. Dent Mater 2018;34:809–18.

[14] Dimitriadi M, Panagiotopoulou A, Pelecanou M, Yannakopoulou K, Eliades G. Stability and reactivity of γ-MPTMS silane in some commercial primer and adhesive formulations. Dent Mater 2018;34:1089–101.

[15] Hooshmand T, van Noort R, Keshvad A. Bond durability of the resin-bonded and silane treated ceramic surface. Dent Mater 2002;18:179–88.

[16] Foxton RM, Nakajima M, Tagami J, Miura H. Effect of acidic pretreatment combined with a silane coupling agent on bonding durability to silicon oxide ceramic. J Biomed Mater Res B Appl Biomater 2005;73:97–103.

[17] Lundvall PK, Ruyter E, Rønold HJ, Ekstrand K. Comparison of different etching agents and repair materials used on feldspathic porcelain. J Adhes Sci Technol 2009;23:1177–86.

[18] Queiroz JR, Souza RO, Nogueira Junior Jr L, Ozcan M, Bottino MA. Influence of acid-etching and ceramic primers on the repair of a glass ceramic. Gen Dent 2012;60:e79–85.

[19] Nishiyama N, Horie K, Asakura T. Hydrolysis and condensation mechanisms of a silane coupling agent studied by ^{13}C and ^{29}Si NMR. J Appl Polym Sci 1987;34:1619–30.

[20] Mahmoud MM, Folz DC, Suchicital C, Clark DE. Estimate of the crystallization volume fraction in lithium disilicate glass-ceramics using Fourier transform infrared reflectance spectroscopy. J Eur Ceram Soc 2015;35:597–604.

[21] Suzdaltsev EI, Borodai SP, Khamitsaev AS, Kharitonov DV. IR spectroscopy study of pre-crystallization and its effect on the phase composition of lithium aluminosilicate glass and glass ceramic. Refract Ind Ceram 2004;45:19–24.

[22] Tian R, Seitz O, Li M, Hu W, Chabal YJ, Gao J. Infrared characterization of interfacial Si–O bond formation on silanized flat SiO_2/Si surfaces. Langmuir 2010;26:4563–6.

[23] Glowacky J, Heißler S, Boese M, Leiste H, Koker T, Faubel W, et al. Investigation of siloxane film formation onfunctionalized Germanium crystals by atomic force microscopy and FTIR-ATR spectroscopy. Hydrophobe V 2008:219–32.

[24] Anagnostopoulos T, Eliades G, Palaghias G. Composition, reactivity and surface interactions of three dental silane primers. Dent Mater 1993;9:182–90.

[25] Harrick NJ. Internal reflection spectroscopy. N. York: John Wiley & Sons Inc.; 1967.

[26] Miller JD, Ishida H. Quantitartive analysis of covalent bonding between substituted silanes and inorganic surfaces. J Chem Phys 1987;86:1593–600.

[27] Rodríguez MA, Liso MJ, Rubio F, Rubio J, Oteo JL. Study of thereaction of γ-methacryloxypropyltrimethoxysilane (γ-MPS) with slate surfaces. J Mater Sci 1999;34:3867–73.

[28] Nistal A, Palencia C, Mazo MA, Rubio F, Rubio J, Oteo JL. Analysis of the interaction of vinyl and carbonyl silanes with carbon nanofiber surfaces. Carbon 2011;49:1635–45.

[29] Eliades G, Vougiouklakis G, Palaghias G. Heterogeneous distribution of single-bottle adhesive monomers in the resin–dentin interdiffusion zone. Dent Mater 2001;17:277–83.

[30] Sumino N, Tsubota K, Takamizawa T, Shiratsuchi K, Miyazaki M, Latta MA. Comparison of the wear and flexural characteristics of flowable resin composites for posterior lesions. Acta Odontol Scand 2013;71:820–7.

[31] DeHoff PH, Anusavice KJ, Wang Z. Three-dimensional finite element analysis of the shear bond test. Dent Mater 1995;11(2):126–31.

[32] Foxton RM, Nakajima M, Hiraishi N, Kitasako Y, Tagami J, Nomura S, et al. Relationship between ceramic primer and ceramic surface pH on the bonding of dual-cure resin cement to ceramic. Dent Mater 2003;19:779–89.

[33] Lohbauer U, Zipperle M, Rischka K, Petschelt A, Müller FA. Hydroxylation of dental zirconia surfaces: characterization and bonding potential. J Biomed Mater Res B Appl Biomater 2008;87(2):461–7.

[34] Lim K, Yap AU, Agarwalla SV, Tan KB, Rosa V. Reliability, failure probability, and strength of resin-based materials for CAD/CAM restorations. J Appl Oral Sci 2016;24:447–52.

[35] Chen B, Lu Z, Meng H, Chen Y, Young L, Zhang H, et al. Effectiveness of pre-silanization in improving bond performance of universal adhesives or self adhesive resin cements to silica-based ceramics: chemical and in vitro evidences. Dent Mater 2019;35:543–53.

[36] Pashley DH, Sano H, Ciucchi B, Yoshiyama M, Carvalho RM. Adhesion testing of dentin bonding agents: a review. Dent Mater 1995;11:117–25.

[37] ISO 29022:2013. Dentistry-adhesion-notched-edge shear bond strength. Geneva: International Organization for Standardization; 2013.